# Inelastic neutron scattering studies of doped CeNiSn and CeRhSb: Crystal-field excitations and origin of the pseudogap

J.-Y. So* and S.-J. Oh
*School of Physics and Center for Strongly Correlated Materials Research, Seoul National University, Seoul 151-747, Korea*

J.-G. Park†
*Department of Physics and Institute of Basic Sciences, SungKyunKwan University, Suwon 440-746, Korea and Center for Strongly Correlated Materials Research, Seoul National University, Seoul 151-747, Korea*

D. T. Adroja
*ISIS Facility, Rutherford Appleton Laboratory, Chilton, Didcot OX11 0QX, United Kingdom*

K. A. McEwen
*Department of Physics and Astronomy, University College London, Gower Street, London WC1E 6BT, United Kingdom*

T. Takabatake
*Department of Quantum Matter, ADSM, Hiroshima University, Higashi-Hiroshima 739-8530, Japan*
(Received 5 November 2003; revised manuscript received 11 April 2005; published 30 June 2005)

The formation of pseudogaps in CeNiSn and CeRhSb has been a puzzle for more than a decade. In order to uncover the mystery, we have undertaken inelastic neutron scattering studies of $CeNi_{0.85}Cu_{0.15}Sn$ and $CeRh_{1-x}Pd_xSb$ with $x=0.1$ and 0.2. From this study, we have succeeded in finding two observable crystal field excitations experimentally. Our subsequent analysis using a crystalline electric field (CEF) Hamiltonian reveals that the experimental observation can be explained by two separate solutions of the CEF Hamiltonian with different ground state wave functions. Interestingly enough, these two solutions are the same ones favored by two independent theoretical models. We have made further analysis and calculations using a superposition model in order to distinguish between these two solutions and, furthermore, discuss our findings with respect to the currently available theories. Our new results shed light on the nature of the gap formation of CeNiSn and CeRhSb.

DOI: 10.1103/PhysRevB.71.214441 PACS number(s): 75.30.Mb, 71.70.Ch, 78.70.Nx

## I. INTRODUCTION

Heavy fermion materials containing Ce, Yb, and U atoms display several distinct ground states, whose existence depends crucially on a delicate balance between the competing RKKY and Kondo interactions. Among the possible ground states, there is a so-called low carrier Kondo system, or sometimes dubbed as Kondo semimetal, whose primary bulk properties have been interpreted in terms of often extremely low density of carriers with strong correlation effects. Interestingly, most of the materials belonging to this category of the low carrier density Kondo system appear to share a common cubic structure with the exception of only three examples. This then led to the Aeppli and Fisk conjecture about the origin of such low carrier Kondo behavior,[1] which states that to have as simple a band-crossing as possible at the Fermi level is a necessary condition for having such low carrier density states. The only three exceptions to this seemingly natural rule are CeNiSn, CeRhSb, and CeRhAs. It is intriguing to note that all three share the same orthorhombic $\epsilon$-TiNiSi-type structure.

As low carrier density systems all three compounds with the $\epsilon$-TiNiSi structure show similar features in various physical properties that are in accordance with the picture of a gap opening at the Fermi level. The size of the gap varies from 28 K for CeNiSn to 56 K for CeRhSb to 280 K for CeRhAs.[2] This gap opening was most clearly seen in tunnelling experiments and high resolution photoemission experiments.[3,4] It is also worthwhile to note that a similar gap feature was observed in the spin excitations of CeNiSn as measured by inelastic neutron scattering, thus CeNiSn also has a so-called spin gap.[5,6] Interestingly enough, this spin gap of CeNiSn is strongly $Q$-dependent and, simultaneously, temperature dependent. For example, the spin gap seen in the data taken with $Q=[0,0,1.2]$ appears only below $T=10$ K. This is the coherence temperature obtained from bulk properties, below which the hybridized Ce $4f$ electrons form a Bloch state.

There have since been numerous experimental as well as theoretical studies in order to understand the origin of the gap supposedly opening at the Fermi level in these three Ce compounds with the $\epsilon$-TiNiSi structure, in particular CeNiSn.[7] Despite these extensive and sometimes successful studies, our understanding of the gap opening in the Ce materials remains incomplete and the microscopic mechanism behind the gap formation is still elusive. For example, three independent theoretical scenarios have so far been put forward as possible explanations for the anomalous gap opening in CeNiSn and CeRhSb. One is a so-called spin liquid picture proposed by Kikoin *et al.*[8] According to their explana-

 

tion, the gap arises from a spin fermionic state through strong coupling between heavy quasiparticles and two low lying crystalline electric field (CEF) states of $Ce^{3+}$ ions. Thus, this theory requires an energy splitting between the ground state and the first excited CEF state to be smaller than a characteristic energy scale of CeNiSn, in this case the Kondo temperature $T_K=54$ K. Other proposals invoking different physics were independently made by two groups.[9,11] These latter two theories put a stress on the importance of the $Q$-dependence of the hybridization between the Ce $4f$ electron and the conduction electrons, and, more importantly, require a specific form of the ground state wave function of Ce $4f$ CEF states. However, even these two models disagree about the ground state wave function of Ce $4f$ CEF states required for their respective theories. For example, the Ikeda and Miyake theory[9] suggested that the ground state of Ce $4f$ electrons should be in a pure $|\pm 3/2\rangle$ state. Recently, a similar idea has also been applied to the case of $|\pm 1/2\rangle$ state.[10] On the other hand, the Moreno and Coleman theory[11] found that there exist three global minima and three local minima in the CEF parameter space with small differences in their free energies among the favorable states. It is also to be noted that all three theories seem to be successful at explaining specific, sometimes very subtle, features of experimental findings, so it has been extremely difficult to differentiate among the three models purely based on the bulk properties alone. Unfortunately, inelastic neutron scattering studies, which otherwise could deliver very decisive information towards the above problem, cannot be as useful to efforts of unfolding the problem because of the expected strong hybridization between $4f$ electron and conduction electrons. It is well known that it is often difficult even to measure clear crystal field excitations, let alone to determine the wave function of a ground state, for heavy fermion compounds.[12]

Early attempts including ours that addressed the problem of the ground state wave function of CeNiSn were not very successful[13,14] because the CEF excitations of Ce $4f$ electrons are indeed very broad and, to make things worse, located very close to strong phonon peaks. Nevertheless, our previous experiment using a single crystal CeNiSn (Ref. 14) succeeded in finding one broad CEF excitation around 40 meV. However, we failed to find another CEF excitation expected from the Ce $4f$ electron in the usual CEF scheme mainly because of the strong phonon features appearing at a region of energy where we anticipated another CEF excitation. Similar inelastic neutron experiments have been made on CeRhSb (Refs. 15,16) to find that CeRhSb too shows a broad CEF excitation at about 35 meV, but they failed to locate the second transition in their measured spectra.

In this paper, we present our recent results that studied the CEF excitations of both CeNiSn and CeRhSb, where we deliberately brought the systems toward a more localized regime by doping Cu on the Ni site of CeNiSn and Pd on the Rh site of CeRhSb. From the previous measurements of bulk properties by other groups,[17,18] it has been known that such doping makes Ce $4f$ electrons of CeNiSn and CeRhSb more localized. As we demonstrate below, this forced localization of the $4f$ electrons turned out to be much more helpful to our study of the wave function of the ground state than otherwise would be possible with the parent compounds. In fact, early Pt doped CeNiSn studies by one of us[19] were made in a similar line of thought and proved fruitable.

## II. EXPERIMENTAL DETAILS

For this study, we prepared three polycrystalline samples of $CeNi_{0.85}Cu_{0.15}Sn$ and $CeRh_{1-x}Pd_xSb$ with $x=0.1$ and 0.2 by arc-melting constituent materials. We studied the structure of all the samples before starting inelastic neutron scattering experiments to find that all the samples form in the $\epsilon$-TiNiSn structure. We measured inelastic neutron scattering from $CeNi_{0.85}Cu_{0.15}Sn$ and $CeRh_{1-x}Pd_xSb$ with $x=0.1$ and 0.2 using the HET time-of-flight chopper spectrometer at the ISIS pulsed neutron facility, Rutherford Appleton Laboratory, UK. Measurements were made on powdered samples, each weighing more than 15 g, with incident neutron energies of 23 and 60 meV. The experimental resolution was about 1 and 3 meV for the 4 m detector bank at the elastic position with the incident energies of 23 and 60 meV, respectively. At HET, neutrons are scattered from the sample into two forward detector banks, one at low scattering angle $\phi=2.6^\circ \rightarrow 7.2^\circ$ at a distance of 4 m from the sample position, and a second bank covering the higher scattering angle $\phi=9.3^\circ \rightarrow 28.7^\circ$ at a distance of 2.5 m from the sample. Two more high-angle detector banks are located at 2.5 and 4 m with average scattering angle $\langle\phi\rangle=114.92^\circ$ and $133.38^\circ$, respectively. All our data are given in absolute units of mb $meV^{-1}$ $sr^{-1}$ $f.u.^{-1}$ through an absolute normalization procedure using a standard vanadium sample. In order to estimate phonon contributions in our Ce spectra, we have measured isostructural reference compounds, LaNiSn and LaRhSb, under identical conditions. Since Rh is a strong neutron absorbing element, we have made absorption corrections to our inelastic scattering data of $CeRh_{1-x}Pd_xSb$ with $x=0.1$ and 0.2 using the standard absorption correction method given in the ISIS data analysis program HOMER, which was originally written by Osborn.

## III. RESULTS AND ANALYSIS

Inelastic neutron scattering intensity from the low angle detector banks at HET measures directly both phonon and magnetic excitations of a system over a thermal energy range, while that from the high angle detector banks gives mostly the phonon contribution. When incident (scattered) neutrons have momentum $\mathbf{k}_i$ ($\mathbf{k}_f$) and energy $E_i$ ($E_f$), the magnetic neutron scattering cross section is given by the following formula:

$$\frac{d^2\sigma}{d\Omega\, d\omega} = \frac{k_f}{k_i} S_{\mathrm{mag}}(\boldsymbol{\kappa}, E),$$

where $S_{\mathrm{mag}}(\boldsymbol{\kappa}, E)$ is given below,

$$S_{\mathrm{mag}}(\boldsymbol{\kappa}, E) = (\gamma r_0)^2 \sum_{\alpha\beta} (\delta_{\alpha\beta} - \tilde{\kappa}_\alpha \tilde{\kappa}_\beta) \sum_{\lambda\lambda'} p_\lambda \langle\lambda|\hat{Q}^+_\alpha|\lambda'\rangle \times \langle\lambda'|\hat{Q}_\beta|\lambda\rangle \delta(E + E_\lambda - E_{\lambda'}), \quad (1)$$

where $\gamma=1.913$, $r_0$ is the classical radius of the electron,

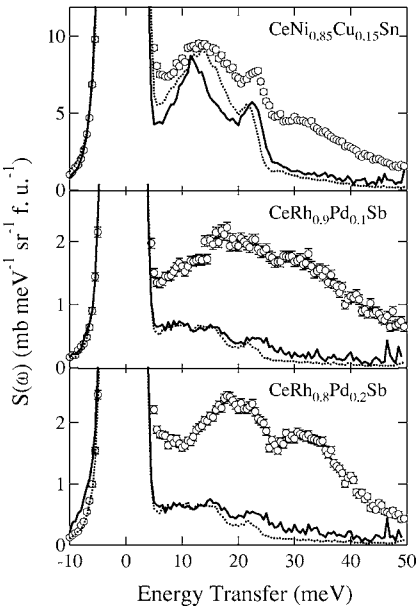


FIG. 1. The data from the low angle detector banks at 2.5 m with $\langle 2\Theta\rangle = 19°$ (open circles) of $CeNi_{0.85}Cu_{0.15}Sn$, $CeRh_{0.9}Pd_{0.1}Sb$, and $CeRh_{0.8}Pd_{0.2}Sb$ taken at 6 K (from top to bottom). The lines are for our estimates of phonon contributions to the low angle data using the ratio method (solid line) and the direct subtraction method (dotted line) (see the text).

$\boldsymbol{\kappa}=\mathbf{k}_i-\mathbf{k}_f$ (momentum transfer), $E=E_i-E_f$ (energy transfer), $p_\lambda$ a thermal occupation of the initial state λ, and $E_\lambda$ and $E_{\lambda'}$ the energies of the initial and final states, respectively. For rare-earth ions that have a large spin-orbit splitting, a dipole approximation gives $\hat{Q} \simeq \frac{1}{2} g F(\kappa)\hat{J}$, where $F(\kappa)$ is a magnetic form factor and $g$ a Landé factor.

Our data taken at 6 K with the incident energy of 60 meV are presented in Fig. 1 for the 2.5 m low angle bank for $CeNi_{0.85}Cu_{0.15}Sn$ and $CeRh_{1-x}Pd_xSb$ with $x=0.1$ and 0.2. These low angle data contain both phonon and magnetic excitations unlike the high angle data (not shown here), which are predominantly from phonon contributions. This difference between the two data sets arises from the fact that in Eq. (1) the magnetic neutron scattering intensity is proportional to the square of the magnetic form factor, $F(\kappa)$. When calculated for an energy transfer of 30 meV with the incident energy of 60 meV, the square of the form factor of $Ce^{3+}$ ion gives a value of 0.795 for the 2.5 m low angle bank with $\langle 2\Theta\rangle = 19°$ and 0.055 for the 2.5 m high angle bank with $\langle 2\Theta\rangle = 133.38°$. On the other hand, the phonon contributions to the scattering intensity of inelastic neutron scattering measurement generally take the following form:[20] $S_{\rm ph}(\kappa,\omega)=a(\omega)+b(\omega)\kappa^2$, where $b(\omega)$ results from single phonon scattering processes and $a(\omega)$ represents multiple-scattering processes that are isotropic to a very good approximation.

There are two methods of estimating the phonon contribution in order to obtain the pure magnetic contributions to the low angle data. One is a so-called ratio method,[21] in which one uses an experimentally measured ratio between the data from the low angle bank and the data from the high angle bank of a nonmagnetic homologue material, referred to as a phonon blank material. In our case, these two nonmagnetic homologue materials are LaNiSn and LaRhSb. One can find more detailed discussions on the so-called ratio method in Ref. 21. In this ratio method, one can deduce the magnetic scattering using the following equation:

$$S^{\rm Ce}_{\rm mag}(\omega) = S^{\rm Ce}_{\rm low}(\omega) - S^{\rm Ce}_{\rm high}(\omega) \times [S^{\rm La}_{\rm low}(\omega)/S^{\rm La}_{\rm high}(\omega)], \quad (2)$$

where $S^{\rm Ce}_{\rm low}(\omega)$ is the low angle scattering data from the Ce compound, $S^{\rm Ce}_{\rm high}(\omega)$ the high angle scattering data from the Ce compound, $S^{\rm Ce}_{\rm mag}(\omega)$ the magnetic contribution, $S^{\rm La}_{\rm low}(\omega)$ the low angle scattering data from the phonon blank sample, and $S^{\rm La}_{\rm high}(\omega)$ the high angle scattering data from the phonon blank sample. Another method is a so-called direct subtraction procedure, in which one uses the low angle data of the La sample as the appropriate phonon contribution to the low angle data of the Ce sample after allowing for the difference in the coherent cross section of La and Ce. In this case, the magnetic contributions to the spectra can be estimated using the following equation:

$$S^{\rm Ce}_{\rm mag}(\omega) = S^{\rm Ce}_{\rm low}(\omega) - \alpha \times S^{\rm La}_{\rm low}(\omega), \quad (3)$$

where $\alpha$ accounts for the difference in the cross section of CeNiSn (CeRhSb) and LaNiSn (LaRhSb). In Fig. 1, we show our phonon estimates as lines for all three Ce compounds using both methods aforementioned. As one can see, both methods work quite well and give very similar phonon estimates for all three systems. In fact, the phonon densities of $CeNi_{0.85}Cu_{0.15}Sn$ are in good agreement with phonon features of pure CeNiSn observed in our previous single crystal experiment.[14] In the following, we used the ratio method to obtain the magnetic contributions. The advantage of this method is that the phonon peaks from the Ce samples have the same energies in both high and low angle banks, compared with a small energy shift incurring between the La and Ce related phonon peaks due to a difference in mass when we use the direct subtraction method. We note one last caution about how we have estimated the magnetic contributions. Although the method just described works very well for magnetic excitations that are well-separated from the elastic line, we found that it is quite tricky and needs cares to estimate the magnetic quasielastic peak correctly for the data taken with the incident energy of $E_i=60$ meV. As a cross-check, we also obtained the magnetic quasielastic scattering from the data taken with $E_i=23$ meV by directly subtracting the elastic peak, where we used the elastic peak function of the standard vanadium data measured under the same conditions. Both magnetic quasielastic structures obtained from the two data sets with $E_i=23$ and 60 meV are in good agreement with one another.

The magnetic scattering data obtained through the ratio method are presented in Fig. 2 for all three Ce compounds after corrections made for the magnetic form factor, $F(\kappa)$. As one can see in the figure, there are two clearly observable peaks around 20 and 35 meV in the magnetic scattering of all three samples. It is worth noting that the peak near 35 meV is the one that we identified in the previous single crystal experiment of CeNiSn.[14] However, the peak around

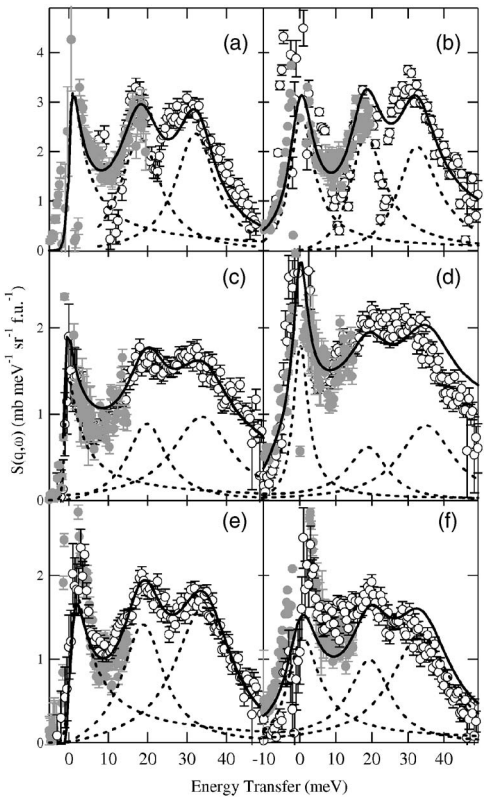


FIG. 2. Magnetic scattering obtained after subtracting phonon contributions off from the raw data for $CeNi_{0.85}Cu_{0.15}Sn$ [(a) 6 K and (b) 100 K], $CeRh_{0.9}Pd_{0.1}Sb$ [(c) 6 K and (d) 100 K], and $CeRh_{0.8}Pd_{0.2}Sb$ [(e) 6 K and (f) 100 K]. Open (closed) symbols are for data taken with $E_i$=60 (23) meV. The solid lines through the data points are our curve fitting results using a CEF Hamiltonian (case I) discussed in the text; the dotted lines are for the quasielastic contribution and the two inelastic peaks. The fitting lines of the 100 K data (b, d, and f) were obtained using the same parameters taken from the analysis of the 6 K data.

20 meV was not previously seen for either CeNiSn or CeRhSb, except for the Pt doped CeNiSn studies.[19]

In order to analyze the magnetic scattering, we considered a CEF Hamiltonian. Before presenting our analysis, we admit that it is not an entirely correct approach for one to use a Hamiltonian based on a localized picture in order to understand Ce compounds, in which the $4f$ electrons are clearly correlated. However, we think that the very observation of well-separated magnetic excitations may well justify our analysis using the CEF Hamiltonian. Furthermore, we are not here claiming that the strongly correlated nature of our Ce systems including the parent compounds CeNiSn and CeRhSb can be solely understood in terms of the Hamiltonian considered below. To the contrary, we note that the specific features of CeNiSn and CeRhSb are due to the combined action of both strongly correlated physics and the CEF Hamiltonian.

As mentioned above, Ce(Ni,Cu)Sn and Ce(Rh,Pd)Sb used in our experiment crystallize in the orthorhombic $Pn2_1a$ space group. The local symmetry of the $Ce^{3+}$ ion can be approximated to have a trigonal $D_{3d}$ symmetry. With this assumption, the CEF Hamiltonian can then be written as follows:[13]

$$H_{\mathrm{CEF}} = B_2^0\hat{O}_2^0 + B_4^0\hat{O}_4^0 + B_4^3\hat{O}_4^3, \tag{4}$$

where $\hat{O}_n^m$ are Stevens' operator equivalents. One notes that for Ce there are no sixth order terms as the corresponding sixth order Stevens factor is zero for $J=5/2$. Under the crystal field, the Hund rules' six degenerate states of $^2F_{5/2}$ for $Ce^{3+}$ are then split into three doublets:

$$a|\pm 1/2\rangle + b|\mp 5/2\rangle, |\pm 3/2\rangle, b|\pm 1/2\rangle - a|\mp 5/2\rangle.$$

While fitting the data against the CEF Hamiltonian, we surveyed very extensive phase spaces of the three $B_2^0$, $B_4^0$, and $B_4^3$ terms with only one constraint of keeping the sign of $B_2^0$ negative. This constraint is consistent with the bulk susceptibility measurements that the magnetic easy axis is the $a$-axis.[22,23] We used a conventional Lorentzian function to fit the quasielastic peak and a damped harmonic oscillator model (DHO) function for the inelastic peaks:[24]

$$S_{\mathrm{inel}}^{\mathrm{DHO}}(E) = \sum_\lambda \frac{A}{1-e^{-E/k_BT}}\left(\frac{1}{(E-E_\lambda)^2+\Gamma_\lambda^2} - \frac{1}{(E+E_\lambda)^2+\Gamma_\lambda^2}\right), \tag{5}$$

where $A_\lambda(\kappa)$ is the relative weight of crystal electric field excitations, $E_\lambda$ the energy of crystalline electric field state, $\Gamma_\lambda$ the linewidth and $(1-e^{-E/k_BT})^{-1}$ a detailed balance factor.

Regardless of starting values, our fitting analysis found that two sets of CEF parameters always give more or less the same goodness of fitting. One set of the parameters has the ground state of $a|\pm 1/2\rangle + b|\mp 5/2\rangle$ with $a$=0.68 and $b$=0.73 for $CeNi_{0.85}Cu_{0.15}Sn$; $a$=0.70 and $b$=0.72 for $CeRh_{0.9}Pd_{0.1}Sb$; $a$=0.79 and $b$=0.61 for $CeRh_{0.8}Pd_{0.2}Sb$ (we refer this state as the MC state) whereas the other produces the ground state of pure $|\pm 3/2\rangle$ (we refer this second state as the IM state). Interestingly enough, the latter state is the one that was favored by the theory of Ikeda and Miyake.[11] A summary of our fitting results are given in Tables I and II. We note that these CEF parameters can explain both the 6 K and 100 K data simultaneously as shown in Fig. 2.

For the CEF parameters giving the MC state (case I in Table I), the ground and second excited states are two doublets of a mixture between $|\pm 1/2\rangle$ and $|\mp 5/2\rangle$, and the first excited state is a doublet of pure $|\pm 3/2\rangle$. It is noticeable that in Table I $B_4^3$ is an order of magnitude larger than $B_2^0$ for case I. The operator $O_4^3$ is the only off-diagonal matrix element in Eq. (4). Therefore, the large value of $B_4^3$ means that the crystal field states are a strong mixture of $|\pm 1/2\rangle$ and $|\mp 5/2\rangle$, as demonstrated by the ground state wave functions. For the CEF parameters producing the IM state (case II in Table I), the ground state is pure $|\pm 3/2\rangle$ doublet while the first and the second excited states are almost pure $|\pm 5/2\rangle$ and $|\pm 1/2\rangle$ with a very little mixing between the two states.

Regarding the general aspects of our data, two points are worth noting. First, all our Ce compounds show significantly well-defined CEF excitations even in the raw data compared with those of pure CeNiSn and CeRhSb,[14–16] indicating that doping Cu and Pd indeed pushes Ce $4f$ electrons towards a more localized regime. Second, when we compare two Pd

TABLE I. CEF parameters: $B_2^0$, $B_4^0$, and $B_4^3$, that are found to give the best fitting results in our analysis. Case I is the set that produces the ground state of a mixture of $|\pm 1/2\rangle$ and $|\mp 5/2\rangle$ while case II leads to the ground state of $|\pm 3/2\rangle$.

| | Case I | | | Case II | | |
|---|---|---|---|---|---|---|
| | $B_2^0$ (meV) | $B_4^0$ (meV) | $B_4^3$ (meV) | $B_2^0$ (meV) | $B_4^0$ (meV) | $B_4^3$ (meV) |
| $CeNi_{0.85}Cu_{0.15}Sn$ | $-0.148$ | $-5.22\times10^{-3}$ | $-1.680$ | $-0.477$ | $9.61\times10^{-2}$ | $-8.21\times10^{-4}$ |
| $CeRh_{0.9}Pd_{0.1}Sb$ | $-8.08\times10^{-2}$ | $-4.84\times10^{-3}$ | $-1.858$ | $-0.505$ | 0.104 | $1.17\times10^{-3}$ |
| $CeRh_{0.8}Pd_{0.2}Sb$ | $-1.91\times10^{-2}$ | $-9.32\times10^{-2}$ | $-1.044$ | $-0.413$ | 0.103 | $-0.162$ |

doped samples, $CeRh_{0.8}Pd_{0.2}Sb$ appears to be more localized than $CeRh_{0.9}Pd_{0.1}Sb$ as seen in the narrower line width of the peaks (see Table II).

Finally, there are two sum rules related to the inelastic neutron scattering data. One concerns the effective moment value: $\int_{-\infty}^{\infty} S_{\mathrm{mag}}(\omega)d\omega = A\mu_{\mathrm{eff}}^2$, where $A = 48.6$ mb sr$^{-1}$ $\mu_B^{-2}$. This allows one to estimate the size of the effective moment involved in the inelastic process.[25] The other is about the uniform bulk susceptibility

$$\int_{-\infty}^{\infty} (1 - e^{-\hbar\omega/k_BT}) \frac{S_{\mathrm{mag}}(\omega)}{\omega} d\omega = \chi'(0),$$

which can be used to calculate the uniform bulk susceptibility using the experimental inelastic neutron data. Note that $S_{\mathrm{mag}}(\omega)$ in the above two expressions and in Fig. 2 is already corrected for the magnetic form factor of $Ce^{3+}$. Using these two sum rules, we calculated the effective moment ($\mu_{\mathrm{eff}}$) and the uniform bulk susceptibility [$\chi'(0)$] by integrating the data from 1.3 to 50 meV. The effective moment of $Ce^{3+}$ ion is 2.56 $\mu_B$ which corresponds to the total cross section of 313.55 mb sr$^{-1}$ $\mu_B^{-2}$ Ce$^{-1}$. However, integration of our data produces only about 40%, 20%, and 23% of the expected total cross section for $CeNi_{0.85}Cu_{0.15}Sn$ (1.02 $\mu_B$), $CeRh_{0.9}Pd_{0.1}Sb$ (0.51 $\mu_B$), and $CeRh_{0.8}Pd_{0.2}Sb$ (0.58 $\mu_B$), respectively. It is typical behavior of heavy fermion compounds that the measured total cross section is smaller than the $Ce^{3+}$ ionic value.[26] From our low temperature data taken at 6 K, we have calculated the following values of the uniform bulk susceptibility: $\chi'(0) = 3.12\times10^{-3}$ emu/mol for $CeNi_{0.85}Cu_{0.15}Sn$, $\chi'(0) = 1.17\times10^{-3}$ emu/mol for $CeRh_{0.9}Pd_{0.1}Sb$, and $\chi'(0) = 1.76\times10^{-3}$ emu/mol for $CeRh_{0.8}Pd_{0.2}Sb$. For comparison, the measured bulk susceptibility values at 6 K are $\chi'(0) = 6.58\times10^{-3}$ emu/mol for $CeNi_{0.85}Cu_{0.15}Sn$,[20] $\chi'(0) = 9.79\times10^{-3}$ emu/mol for $CeRh_{0.9}Pd_{0.1}Sb$, and $\chi'(0) = 24.46\times10^{-3}$ emu/mol for $CeRh_{0.8}Pd_{0.2}Sb$.[27] The discrepancy between the estimated and the measured bulk susceptibility values, we think, is due to the fact that the main focus of our present work is on the magnetic excitations at high energy using thermal neutrons and our data at lower energy, say below 5 meV, inevitably are rather inaccurate. On the other hand, the bulk susceptibility is very sensitive to the lower energy data because of the detailed balance factor and the $\omega$ term in denominator of the above equation we used. An alternative, and more radical explanation, would be that this big discrepancy may simply mean the breakdown of the single ion model we rely on here. Although the latter appears to be a reasonable explanation of some of the difference considering the mixed valence nature of pure CeNiSn and CeRhSb, we cannot tell for sure here how much of the observed difference can be accounted for by this explanation.

## IV. DISCUSSION

As we have studied doped CeNiSn and CeRhSb, one may wonder how relevant our findings in these doped materials are to understanding of the physics of pure CeNiSn and CeRhSb. One particular concern is that as we replace Ni and Rh by Cu and Pd we inevitably disrupt interaction with the ligands that is bound to be different from those of undoped materials. Surely, it is a problem of some concern. However, as we have shown here and previously in Pt doped CeNiSn,[19] the peak position, which is the most important quantity in determining the parameters of crystal field Hamiltonian, does not seem to change too much upon doping at the Ni site of CeNiSn and the Rh site of CeRhSb. Therefore, we maintain that although we cannot disregard the disrupting effects of doping on the ligand site the main findings of our works on doped systems can be largely considered to hold true for the pure CeNiSn and CeRhSb.

Before going further into details of our analysis, we like to stress that there are two clearly well-defined CEF excita-

TABLE II. Location of the two inelastic peaks for the two sets of the CEF parameters (see the text). $\Gamma_1$ and $\Gamma_2$ represent full width at half maximum (FWHM) of the two peaks. I and II inside the parentheses indicate which set of the CEF parameters in Table I the values are given for.

| | $E_1$ (meV) (I) | $E_2$ (meV) (I) | $E_1$ (meV) (II) | $E_2$ (meV) (II) | $\Gamma_1$ (meV) | $\Gamma_2$ (meV) |
|---|---|---|---|---|---|---|
| $CeNi_{0.85}Cu_{0.15}Sn$ | 17.83 | 31.96 | 16.92 | 31.71 | 4.56 | 6.80 |
| $CeRh_{0.9}Pd_{0.1}Sb$ | 19.19 | 35.18 | 18.86 | 34.18 | 6.42 | 9.24 |
| $CeRh_{0.8}Pd_{0.2}Sb$ | 20.49 | 35.45 | 19.71 | 33.69 | 6.00 | 8.91 |

tions at around 20 and 35 meV for all three Ce compounds in our experimental data. (Please note that a maximum of two CEF excitations can be expected in the magnetic scattering from a $Ce^{3+}$ ion.) Therefore the energy splitting ($\Delta_{CF}$) between the ground and the first excited states are 20 meV for all our samples, which is larger than the Kondo temperature, $T_K$, of both CeNiSn and CeRhSb; $T_K$=54 K for CeNiSn and $T_K$=96 K for CeRhSb.[28] This is in sharp contrast with the theory of Kikoin *et al.*,[8] which requires the energy splitting ($\Delta_{CF}$) to be smaller than $T_K$. This then rules out the so-called spin liquid theory as an explanation for the pseudo-gap behavior of CeNiSn.

Unfortunately, however, the two solutions of the CEF parameters we obtained, thus two sets of CEF level schemes, cannot be distinguished by our data and subsequent fitting with the CEF Hamiltonian alone. Nevertheless, it is very interesting to note that the two solutions we found are exactly the same ones that are favored by theories.[9,11] As one can see in Table I, a main difference between the two solutions is the relative strength of $B_4^3$ with respect to other two terms in the Hamiltonian. For example, the CEF parameters with $|\pm 3/2\rangle$ as the ground state (case II in Table I) have a much smaller $B_4^3$ term than those with the ground state of $a|\pm 1/2\rangle + b|\mp 5/2\rangle$.

In order to gain insight into the problem of the ground state wave function, we have made theoretical calculations based on a superposition model.[29,30] Although we acknowledge that one should use the superposition model with caution in the studies of strongly correlated electron systems, we believe that it can be used at least as a guide when one analyzes inelastic neutron scattering data using a CEF Hamiltonian. According to our calculations using the superposition model, it appears that the $B_4^3$ term is always larger than the $B_4^0$ term.[31] Similar results were previously obtained for YbNiSn with the same $\epsilon$-TiNiSn structure too.[32] This indicates that the ground state of $a|\pm 1/2\rangle + b|\mp 5/2\rangle$ is likely to be more favorable than that of $|\pm 3/2\rangle$.

Last, but not the least, we like to note that previous studies found similarly narrow inelastic peaks in some of mixed valent compound. For example, $SmB_6$ was found to show a very narrow excitation centered around 14 meV, which is anisotropic and strongly temperature dependent.[33] Although we admit that it is intriguing to compare our observations in doped CeNiSn and CeRhSb with those of $SmB_6$, there is striking difference between the two that is the temperature dependence. Unlike $SmB_6$, we found in Fig. 2 that the temperature dependence of the excitations of our doped systems can be best described by the usual temperature dependence of the crystal field excitations.

## V. CONCLUSIONS

To summarize, we have measured the inelastic neutron scattering of $CeNi_{0.85}Cu_{0.15}Sn$ and $CeRh_{1-x}Pd_xSb$ with $x$ =0.1 and 0.2 in order to investigate the ground state of $Ce^{3+}$ ion. In our data, we succeeded in finding clearly visible magnetic excitations centered around 20 and 35 meV, which we ascribe to excitations due to the CEF levels of $Ce^{3+}$ ion. Our analysis based on a CEF Hamiltonian shows that there exist two stable solutions that can account for the data. One solution gives the ground state of $a|\pm 1/2\rangle + b|\mp 5/2\rangle$ while the other has the ground state of pure $|\pm 3/2\rangle$. These two solutions are in fact favored by two independent theoretical studies[9,11] that reproduced bulk properties successfully. We subsequently made further analysis using a superposition model to find that the solution with the ground state of $a|\pm 1/2\rangle + b|\mp 5/2\rangle$ is more favorable than the other.

## ACKNOWLEDGMENTS

We thank Professor M. Kohgi for lending us the LaRhSb sample used in this work. Experiments at ISIS were supported by the Engineering and Physical Sciences Research Council of the U.K. Work at SungKyunKwan University was supported by the Korea-UK collaborative research and the Proton Accelerator User Program (No. M102KS010001-02K1901-01810) of Proton Engineering R & D Project of the Ministry of Science and Technology. We (J.Y.S., J.G.P., and S.J.O.) acknowledge financial support of the Center for Strongly Correlated Materials Research.

*Present address: Neutron Physics Department, Korea Atomic Energy Research Institute, Daejeon 305-600, Korea.

†Electronic address: jgpark@skku.edu; Permanent address: Department of Physics, SungKyunKwan University, Suwon 440-746, Korea.

[1] G. Aeppli and Z. Fisk, Comments Condens. Matter Phys. **16**, 155 (1992).

[2] T. Takabatake, T. Sasakawa, J. Kitagawa, T. Suemitsu, Y. Echizen, K. Umeo, and Y. Bando, Physica B **328**, 53 (2003).

[3] T. Ekino, T. Takabatake, H. Tanaka, and H. Fujii, Phys. Rev. Lett. **75**, 4262 (1995).

[4] H. Kumigashira, T. Takahashi, S. Yoshii, and M. Kasaya, Phys. Rev. Lett. **87**, 067206 (2001).

[5] T. E. Mason, G. Aeppli, A. P. Ramirez, K. N. Clausen, C. Broholm, N. Stücheli, E. Bucher, and T. T. M. Palstra, Phys. Rev. Lett. **69**, 490 (1992).

[6] T. J. Sato, H. Kadowaki, H. Yoshizawa, T. Ekino, T. Takabatake, H. Fujii, L. P. Regnault, and Y. Isikawa, J. Phys.: Condens. Matter **7**, 8009 (1995).

[7] *For review, see* P. S. Riseborough, Adv. Phys. **49**, 257 (2000), and references therein.

[8] K. A. Kikoin, M. N. Kiselev, A. S. Mishchenko, and A. de Visser, Phys. Rev. B **59**, 15070 (1999).

[9] H. Ikeda and K. Miyake, J. Phys. Soc. Jpn. **65**, 1769 (1996).

[10] M. Miyazawa and K. Yamada, J. Phys. Soc. Jpn. **72**, 2033 (2003).

[11] J. Moreno and P. Coleman, Phys. Rev. Lett. **84**, 342 (2000).

[12] E. Holland-Moritz and G. H. Lander, in *Handbook on the Physics and Chemistry of Rare Earths*, edited by K. A. Gschneidner, Jr., L. Eyring, G. H. Lander, and G. R. Choppin (Elsevier Science

B. V., Amsterdam, 1994), Vol. 19, Chap. 130.

[13] P. A. Alekseev, E. S. Klement'ev, V. N. Lazukov, E. V. Nefedova, I. P. Sadikov, A. Yu. Muzychka, I. L. Sashin, N. N. Efremova, and W. Bührer, JETP **79**, 665 (1994); M. Kohgi, K. Ohoyama, T. Osakabe, M. Kasaya, T. Takabatake, and H. Fujii, Physica B **186-188**, 409 (1993).

[14] J.-G. Park, D. T. Adroja, K. A. McEwen, Y. J. Bi, and J. Kulda, Phys. Rev. B **58**, 3167 (1998).

[15] K. Ohoyama, M. Kohgi, Y. Yoshino, T. Takabatake, W. Hahn, and R. S. Eccleston, Physica B **259–261**, 283 (1999).

[16] L. Menon, D. T. Adroja, B. D. Rainford, S. K. Malik, and W. B. Yelon, Solid State Commun. **112**, 85 (1999).

[17] L. Menon, F. E. Kayzel, A. de Visser, and S. K. Malik, Phys. Rev. B **58**, 85 (1998).

[18] G. M. Kalvius, A. Kratzer, G. Grosse, D. R. Noakes, R. Wäppling, H. v. Löhneysen, T. Takabatake, and Y. Echizen, Physica B **289–290**, 256 (2000).

[19] D. T. Adroja, B. D. Rainford, A. J. Neville, and A. G. M. Jansen, Physica B **223&224**, 275 (1996).

[20] D. T. Adroja, B. D. Rainford, J. M. deTeresa, A. delMoral, M. R. Ibarra, and K. S. Knight, Phys. Rev. B **52**, 12790 (1995).

[21] A. P. Murani, Phys. Rev. B **28**, 2308 (1983).

[22] T. Yoshino, Y. Echizen, T. Takabatake, and M. Sera, Physica B **281&282**, 291 (2000).

[23] G. Nakamoto, T. Takabatake, H. Fujii, A. Minami, K. Maezawa, I. Oguro, and A. A. Monovsky, J. Phys. Soc. Jpn. **64**, 4834 (1995).

[24] J. W. Halley and R. Hastings, Phys. Rev. B **15**, 1404 (1977), where dampled harmonic oscillator (DHO) function was used to analyze inelastic neutron spectrum of liquid $^4$He. For the present studies, we used the DHO function to fit the inelastic peak as it satisfies the detailed balanced factor and, at the same time, has a better behaved tail than the usual Lorentzian function. For the quasielastic response, we used a Lorentzian function that is the response function of a spin system having an exponential temporal decay.

[25] J.-G. Park, K. A. McEwen, and M. J. Bull, Phys. Rev. B **66**, 094502 (2002).

[26] A. P. Murani, A. Severing, and W. G. Marshall, Phys. Rev. B **53**, 2641 (1996).

[27] D. T. Adroja (unpublished, 2005).

[28] T. Takabatake, F. Teshima, H. Fujii, S. Nishigori, T. Suzuki, T. Fujita, Y. Yamaguchi, J. Sakurai, and D. Jaccard, Phys. Rev. B **41**, 9607 (1990); T. Takabatake, H. Tanaka, Y. Bando, H. Fujii, S. Nishigori, T. Suzuki, T. Fujita, and G. Kido, *ibid.* **50**, 623 (1994).

[29] D. J. Newman and B. Ng, Rep. Prog. Phys. **52**, 699 (1989).

[30] The superposition model assumes that the CEF parameters can be determined by summing contributions from each ligand. In this model, the CEF parameter $B_n^m$ can be expressed as $B_n^m = \Sigma_j \overline{B_n}(r, R_j) K_{nm}(\theta_j, \phi_j)$, where $\overline{B_n}$ is an intrinsic parameter and $K_{nm}$ a geometrical factor depending purely on angular coordinations of surrounding ions. Thus one can compare the magnitude of the CEF parameters with the same order only by considering the geometrical factor.

[31] J.-Y. So, Ph.D. thesis, Seoul National University (2004).

[32] D. T. Adroja, B. D. Rainford, and T. Takabatake, Physica B **253**, 269 (1998).

[33] P. A. Alekseev, J.-M. Mignot, J. Rossat-Mignod, V. N. Lazukov, I. P. Sadikov, E. S. Konovalova, and Yu B. Paderno, J. Phys.: Condens. Matter **7**, 289 (1995).